World Academy of Science, Engineering and Technology
International Journal of Electronics and Communication Engineering
Vol:10, No:1, 2016

Impulsive Noise-Resilient Subband Adaptive Filter

Young-Seok Choi

Abstract—We present a new subband adaptive filter (R-SAF) which is robust against impulsive noise in system identification. To address the vulnerability of adaptive filters based on the L_2-norm optimization criterion against impulsive noise, the R-SAF comes from the L_1-norm optimization criterion with a constraint on the energy of the weight update. Minimizing L_1-norm of the *a posteriori* error in each subband with a constraint on minimum disturbance gives rise to the robustness against the impulsive noise and the capable convergence performance. Experimental results clearly demonstrate that the proposed R-SAF outperforms the classical adaptive filtering algorithms when impulsive noise as well as background noise exist.

Keywords—Subband adaptive filter, L_1-norm, system identification, robustness, impulsive interference.

I. Introduction

ADAPTIVE filtering has been of considerable interest among various signal processing fields such as channel equalization, system identification, acoustic echo cancellation, and so on. Among a number of adaptive filtering algorithms, the normalized least square (NLMS) algorithm has been preferred due to its simplicity of implementation [1][2]. However, the NLMS suffers from the degradation of convergence in case of a correlated input signal. To overcome this limitation, adaptive filtering in the subband has been recently developed, referred to as the subband adaptive filters (SAFs) [3]–[5]. The remarkable feature of the SAF is that it allocates an input signal and a desired response into almost mutually exclusive subbands. By carrying out a pre-whitening on the correlated input signal, the SAF achieves the improved convergence rate over the fullband based LMS-type filters. Recently, through a multiple-constraints optimization problem based on the principle of minimal disturbance, the normalized SAF (NSAF) has been developed with the superior convergence rate over the NLMS, while it has nearly same computational burden with the NLMS.

Consider that impulsive noise is existent under a system identification scenario such as echo cancellation. Since impulsive noise with non-Gaussian distribution leads to more perturbation rather than Gaussian noise, the convergence behavior of an adaptive filter based on L_2-norm optimization is heavily impaired. To address this issue, several adaptive filtering algorithms which utilize lower order norms have been developed [6]–[8]. Among them, the L_1-norm optimization yields the robustness as well as the simplicity of implementation [7][8]. However, the poor convergence of the adaptive filters based on the L_1-norm optimization in the case of correlated input signals remains as a major drawback. More recently, an affine projection algorithm based on a L_1-norm optimization has been introduced [9].

Y.-S. Choi is with the Department of Electronic Engineering, Gangneung-Wonju National University, 7 Jukheon-gil, Gangneung, 210-702 Republic of Korea (phone: +82-33-640-2429; fax: +82-33-646-0740; e-mail: yschoi@gwnu.ac.kr).

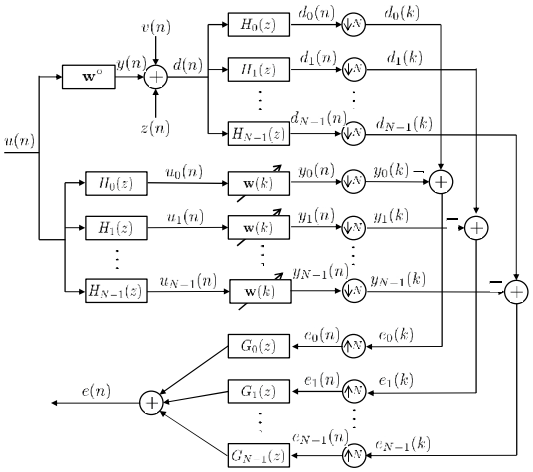

Fig. 1 Subband structure with the analysis filter and synthesis filter and the subband desired signals, subband filter outputs, and subband error signals

Here, to tackle the robustness and convergence behavior issues in subband framework, a new robust SAF (R-SAF) which comes from the L_1-norm optimization criterion is presented. Formulating the L_1-norm of the *a posteriori* error in each subband with a constraint of the energy of the weight update as the cost function and minimizing this cost function, it results in the robust and capable update recursion of the R-SAF. This letter deals with the robustness issue against impulsive interference with non-Gaussian distribution. Furthermore, the novelty of this work lies in the improved convergence compared to conventional L_1-norm based adaptive filters. Through various simulations, the resulting R-SAF has proven its superior robustness and convergence performance over the classical NLMS and the normalized sign algorithm (NSA) [7] in cases when impulsive noise exists.

II. Robust SAF (R-SAF)

Consider a desired signal $d(n)$ that arise from the system identification model

$$d(n) = \mathbf{u}(n)\mathbf{w}^\circ + v(n), \tag{1}$$

where $\mathbf{w}^\circ$ is a column vector for the impulse response of an unknown system that we wish to estimate, $v(n)$ accounts for measurement noise with zero mean and variance σ_v^2 and $\mathbf{u}(n)$ denotes the $1 \times M$ input vector,

$$\mathbf{u}(n) = [u(n)\ \ u(n-1)\ \ \cdots u(n-M+1)]. \tag{2}$$

A. Structure of SAF

Fig. 1 shows the structure of the well known NSAF, where the desired signal $d(n)$ and output signal $y(n)$ are partitioned into N subbands by the analysis filters $H_0(z), H_1(z), \ldots, H_{N-1}(z)$. The resulting subband signals, $d_i(n)$ and $y_i(n)$ for $i = 0, 1, \ldots, N-1$, are critically decimated to a lower sampling rate commensurate with their bandwidth. Here, the variable n to index the original sequences, and k to index the decimated sequences are used for all signals. Then, the decimated filter output signal at each subband is defined as $y_i(k) = \mathbf{u}_i(k)\mathbf{w}(k)$, where $\mathbf{u}_i(k)$ is $1 \times M$ row vector such that

$$\mathbf{u}_i(k) = [u_i(kN), u_i(kN-1), \ldots, u_i(kN-M+1)]$$

and $\mathbf{w}(k) = [w_0(k), w_1(k), \ldots, w_{M-1}(k)]^T$ denotes an estimate for $\mathbf{w}^\circ$ with length M. Then, the *a priori* and *a posteriori* errors at each subband $\{e_{a,i}(k), e_{p,i}(k)\}$ are defined by

$$e_{a,i}(k) = d_i(k) - \mathbf{u}_i(k)\mathbf{w}(k), \tag{3}$$

and

$$e_{p,i}(k) = d_i(k) - \mathbf{u}_i(k)\mathbf{w}(k+1), \tag{4}$$

where $d_i(k) = d_i(kN)$ is the decimated desired signal at each subband for $i = 0, 1, \ldots, N-1$. Then, the *a priori* and *a posteriori* error vectors $\{\mathbf{e}_a(k), \mathbf{e}_p(k)\}$ can be formulated as

$$\mathbf{e}_a(k) = \begin{bmatrix} e_{a,0}(k) \\ e_{a,1}(k) \\ \vdots \\ e_{a,N-1}(k) \end{bmatrix}, \quad \mathbf{e}_p(k) = \begin{bmatrix} e_{p,0}(k) \\ e_{p,1}(k) \\ \vdots \\ e_{p,N-1}(k) \end{bmatrix}.$$

B. Derivation of the R-SAF

Here, the proposed optimization criterion is formulated as follows: Minimizing the L_1-norm of the *a posteriori* error vector

$$\min_{\mathbf{w}(k+1)} \|\mathbf{e}_p(k)\|_1 \tag{5}$$

subject to a constraint on the energy of the filter update, which is given by

$$\|\mathbf{w}(k+1) - \mathbf{w}(k)\|_2^2 \leq \mu^2, \tag{6}$$

where μ^2 denotes a control parameter which prevents the weight update from the abrupt change. The constraint (6) plays a role in restricting the effect of the perturbation, which is based on the principle of minimum disturbance. In this regard, the parameter, μ, needs to be small. Then, the constrained optimization criterion with the Lagrange multiplier is given by as follows:

$$J(k) = \|\mathbf{e}_p(k)\|_1 + \lambda[\|\mathbf{w}(k+1) - \mathbf{w}(k)\|_2^2 - \mu^2], \tag{7}$$

where λ is a Lagrange multiplier. Note that the L_1-norm is a non-differentiable convex function, the gradient does not exist at any point. To deal with this situation, a subgradient method [10] is incorporated. Taking the gradient of (7) with respect to the weight vector $\mathbf{w}(k+1)$, it leads to

$$\begin{aligned} \nabla_{\mathbf{w}(k+1)} J(k) &= \nabla^S_{\mathbf{w}(k+1)} \|\mathbf{e}_p(k)\|_1 + 2\lambda[\mathbf{w}(k+1) - \mathbf{w}(k)]^T \\ &= [\nabla \mathbf{e}_p(k)]^T \mathrm{sgn}(\mathbf{e}_p(k)) + 2\lambda[\mathbf{w}(k+1) - \mathbf{w}(k)]^T \\ &= -\sum_{i=0}^{N-1} \mathrm{sgn}[e_{p,i}(k)]\mathbf{u}_i(k) + 2\lambda[\mathbf{w}(k+1) - \mathbf{w}(k)]^T, \end{aligned} \tag{8}$$

where $\nabla^S_{\mathbf{w}(k+1)} f(\cdot)$ denotes a subgradient vector of a function $f(\cdot)$ with respect to $\mathbf{w}(k+1)$ and $\mathrm{sgn}(\cdot)$ represents the signum function. Setting (8) equal to zero, the following is obtained

$$\mathbf{w}(k+1) = \mathbf{w}(k) + \frac{1}{2\lambda} \sum_{i=0}^{N-1} \mathbf{u}_i^T(k)\mathrm{sgn}[e_{p,i}(k)]. \tag{9}$$

Substituting (9) into the constraint (6), it results in

$$\frac{1}{2\lambda} = \frac{\mu}{\sqrt{\sum_{i=0}^{N-1} \mathrm{sgn}[e_{p,i}(k)]\mathbf{u}_i(k) \cdot \sum_{i=0}^{N-1} \mathbf{u}_i^T(k)\mathrm{sgn}[e_{p,i}(k)]}}. \tag{10}$$

Assuming that the *a priori* error $e_{a,i}(k)$ approximates the *a posteriori* error $e_{p,i}(k)$ and substituting (10) into (9), the proposed R-SAF updates the weight as follows:

$$\mathbf{w}(k+1) = \mathbf{w}(k) + \mu \frac{\sum_{i=0}^{N-1} \mathbf{u}_i^T(k)\mathrm{sgn}[e_{a,i}(k)]}{\sqrt{\sum_{i=0}^{N-1} \mathrm{sgn}[e_{a,i}(k)]\mathbf{u}_i(k) \cdot \sum_{i=0}^{N-1} \mathbf{u}_i^T(k)\mathrm{sgn}[e_{a,i}(k)]}}, \tag{11}$$

where μ plays a role in controlling the convergence as a step-size parameter.

III. Experimental Results

To validate the performance of the proposed R-SAF, computer simulations are carried out in a system identification scenario in which the unknown channel is randomly generated. The length of the unknown system is $M = 128$ in experiments. The adaptive filter and the unknown system are assumed to have the same number of taps. The input signals $u(n)$ are obtained by filtering a white, zero-mean, Gaussian random sequence through a first-order system $G(z) = 1/(1 - 0.9z^{-1})$. The measurement noise $v(n)$ with white Gaussian distribution is added to the system output $y(n)$ such that the signal-to-noise ratio (SNR) is 30 dB, where the SNR is defined as SNR $= 10\log_{10}(E[y^2(i)]/E[v^2(i)])$, where $y(n) = \mathbf{u}(n)\mathbf{w}^\circ$. Impulsive noise $z(n)$ is added to the system output $y(n)$ with the signal-to-interference ratio (SIR) of -30, -10, and 10 dB. This impulsive noise is modeled by a Bernoulli-Gaussian (BG) distribution [11], which is obtained as the product of a Bernoulli distribution and a Gaussian one, i.e., $z(n) = \omega(n)\eta(n)$, where $\omega(n)$ is a Bernoulli process with a probability mass function given by $P(\omega) = 1 - p$ for $\omega = 0$ and $P(\omega) = p$ for $\omega = 1$. The average power of the BG distribution is $p \cdot \sigma_\eta^2$. When keeping the average power constant, the smaller p value, the spikier the BG interference. Here, $p = 0.001$ is used in the simulations except Fig. 7 where various p values are considered. In addition, $\eta(n)$ is additive

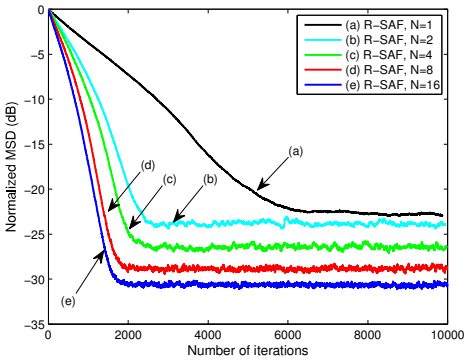

Fig. 2 Normalized MSD curves of the R-SAF with the different number of subbands, $N = 1$, 2, 4, 8, and 16. The interference is the BG process with SIR=-30 dB

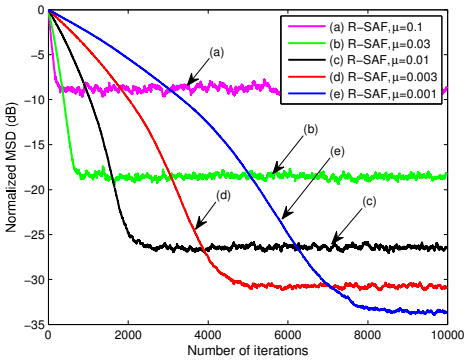

Fig. 3 Normalized MSD curves of the R-SAF with the different step-sizes, $\mu = 0.1$, 0.03, 0.01, 0.003, and 0.001. The interference is a BG process with SIR=-30 dB

white Gaussian noise with zero mean and variance σ_η^2. In order to compare the convergence performance, the normalized mean square deviation (MSD),

$$\text{Normalized MSD} = \text{E}\left(\frac{\|\mathbf{w}^\circ - \mathbf{w}(k)\|^2}{\|\mathbf{w}^\circ\|^2}\right),$$

is taken and averaged over 50 independent trials. The cosine-modulated filter banks [5] with the subband numbers of $N = 1$, 2, 4, 8, and 16 are used in the simulations. The prototype filter of length $L = 32$ is used.

Fig. 2 shows the normalized MSD curves of the R-SAF in cases of the different number of subbands, i.e., N=1, 2, 4, 8, and 16. The step-size, $\mu = 0.01$, SIR=-30 dB, and $p = 0.001$ are used. In the figure, the higher the number of subbands, the better the convergence behavior of the R-SAF in terms of the convergence rate and the steady-state misalignment.

Fig. 3 depicts the convergence performance of the R-SAF with various step-sizes for $N = 4$, where $\mu = 0.1$, 0.03, 0.01, 0.003, and 0.001 are chosen. The same values of SIR and p as those in Fig. 2 are chosen. As expected, the use of a large step-size leads to faster convergence with higher steady-state misalignment. On the contrary, a small step-size reduces the convergence rate, but achieves the lower steady-state misalignment.

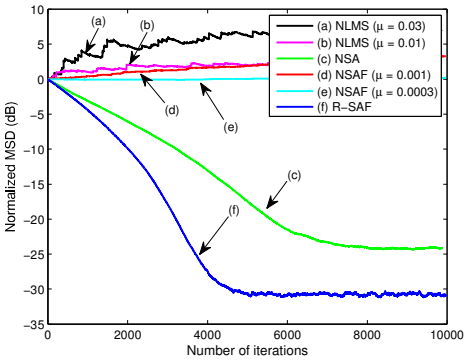

Fig. 4 Normalized MSD curves of the NLMS, NSA, NSAF, and R-SAF under SIR=-30 dB

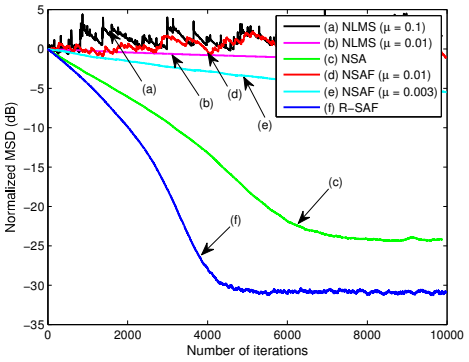

Fig. 5 Normalized MSD curves of the NLMS, NSA, NSAF, and R-SAF under SIR=-10 dB

Figs. 4-6 illustrate the normalized MSD curves of the NLMS, NSA, NSAF, and R-SAF in cases of SIR=-30, -10, and 10 dB, respectively. The number of subbands, N=4, for the NSAF and R-SAF is chosen in these simulations. The step-sizes, $\mu = 0.1$ for the NSA and $\mu = 0.003$ for the R-SAF are used. While the NLMS and the NSAF are vulnerable against impulsive noise, the NSA and the R-SAF are capable of coping with the BG interference. Moreover, the convergence behavior of the R-SAF is superior to that of the NSA.

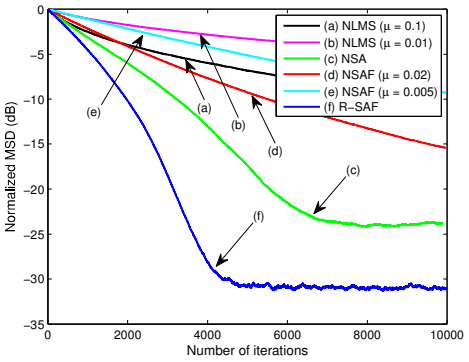

Fig. 6 Normalized MSD curves of the NLMS, NSA, NSAF, and R-SAF under SIR=10 dB

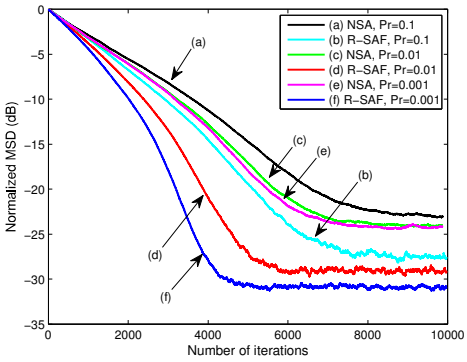

Fig. 7 Normalized MSD curves of the NSA and R-SAF under different p values, $p = 0.1$, 0.01, and 0.001.

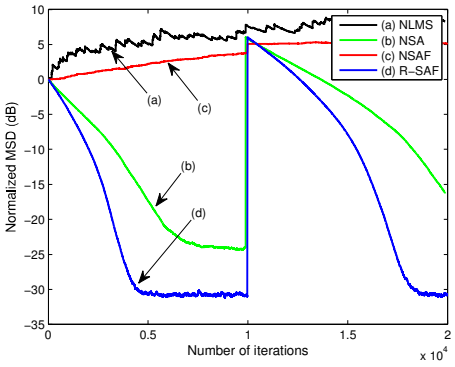

Fig. 8 Normalized MSD curves of the NLMS, NSA, NSAF, and R-SAF in case of a time-varying unknown system. The system is suddenly changed from $\mathbf{w}^\circ$ to $-\mathbf{w}^\circ$ at the 10000th iteration

To examine the effect of the impulsiveness of the BG interference, the convergence performances of the NSA and the R-SAF with $N = 4$ are compared, where $p = 0.1$, 0.01, and 0.001 are considered. The step-sizes are same as those in Figs. 4-6. The SIR is set to -10 dB. It can be seen that the NSA and the R-SAF perform better in cases when the BG interference is more spiky. In addition, the R-SAF achieves highly improved convergence performance over the NSA for all cases.

Finally, the tracking capabilities of the NLMS, NSA, NSAF, and R-SAF to a sudden change in the system are tested. For the SAFs, the number of subbands, $N = 4$, is used. Fig. 8 shows the results of suddenly multiplying the unknown system by -1 at the 10000th iteration. Same values of the step-size in Fig. 4 are used for algorithms. As can be shown, the R-SAF keeps track of weight change without losing the convergence rate nor the steady-state misalignment compared to conventional algorithms.

IV. Conclusion

A robust SAF which stems from a L_1-norm optimization criterion based on subband structure has been dealt with on both robustness and convergence. The resulting R-SAF inherits robustness by utilizing a L_1-norm optimization as well as the capable convergence due to subband framework. A number of numerical simulations have shown that the R-SAF successfully addresses both vulnerability against impulsive interference and poor convergence of the sign algorithm.

References

[1] S. Haykin, *Adaptive Filter Theory*, 4th edition, Upper Saddle River, NJ: Prentice Hall, 2002.
[2] A. H. Sayed, *Fundamentals of Adaptive Filtering*, New York: Wiley, 2003.
[3] A. Gilloire and M. Vetterli, "Adaptive filtering in subbands with critical sampling: analysis, experiments, and application to acoustic echo cancellation," *IEEE Trans. Signal Process.*, vol. 40, no. 8, pp. 1862–875, Aug. 1992.
[4] S. S. Pradhan and V. U. Reddy, "A new approach to subband adaptive filtering," *IEEE Trans. Signal Process.*, vol. 47, no. 3, pp. 655–664, Mar. 1999.
[5] K. A. Lee and W. S. Gan, "Improving convergence of the NLMS algorithm using constrained subband updates," *IEEE Signal Processing Lett.*, vol. 11, no. 9, pp. 736–739, Sept. 2004.
[6] M. Shao and C. L. Nikias, "Signal processing with fractional lower order moments: Stable process and their applications," *Proc. IEEE*, vol. 81, pp. 986–1010, Jul. 1993.
[7] O. Arikan, A. E. Cetin, and E. Erzin, "Adaptive filtering for non-Gaussian stable processes," *IEEE Signal Processing Lett.*, vol. 1, no. 11, pp. 163–165, Nov. 1994.
[8] E. Eweda, "Convergence analysis of the sign algorithm without the independence and Gaussian assumptions," *IEEE Trans. Signal Process.*, vol. 48, no. 9, pp. 2535–2544, Sep. 2000.
[9] T. Shao, Y. R. Zheng, J. Benesty, "An affine projection sign algorithm robust against impulsive interferences," *IEEE Signal Process. Lett.*, vol. 17, no. 4, pp. 327–330, 2010.
[10] D. Bertsekas, A. Nedic, and A. Ozdaglar, *Convex analysis and optimization*, Athena Scientific, Cambridge, USA, 2003.
[11] L. R. Vega, H. Ray, J. Benesty, and S. Tressens, "A new robust variable step-size NLMS algorithm," *IEEE Trans. Signal Process.*, vol. 56, no. 5, pp. 1878-1893, May 2008.